Journal of Alloys and Compounds 586 (2014) 542–548

Contents lists available at ScienceDirect

Journal of Alloys and Compounds

journal homepage: www.elsevier.com/locate/jalcom

Intrinsic relationship between crystallization mechanism of metallic glass powder and microstructure of bulk alloys fabricated by powder consolidation and crystallization of amorphous phase

C. Yang *, L.H. Liu, Y.G. Yao, Y.H. Li, Y.Y. Li

National Engineering Research Center of Near-net-shape Forming for Metallic Materials, South China University of Technology, Guangzhou 510640, People's Republic of China

ARTICLE INFO

Article history:
Received 17 August 2013
Received in revised form 25 September 2013
Accepted 26 September 2013
Available online 10 October 2013

Keywords:
Metallic glass
Crystallization mechanism
Microstructure
Mechanical property
Powder metallurgy

ABSTRACT

$Ti_{64}Nb_{12}Cu_{11.2}Ni_{9.6}Sn_{3.2}$ bulk alloys were fabricated by consolidation of metallic glass (MG) powder synthesized by mechanical alloying and crystallization of amorphous phase. The Johnson–Mehl–Avrami–Kolmogorov method was employed to investigate non-isothermal crystallization kinetic of the synthesized MG powder. The average local Avrami exponent n determined from crystallization kinetic increases from 1.7 to 2.9 and then decreases to 1.8–2.0 when the crystallized volume fraction α is in the range of 0.1–0.3, and around 0.5 and 0.9, respectively. This indicates the corresponding crystallization mechanism is diffusion-controlled three-dimensional growth of nuclei with decreasing nucleation rate, volume diffusion-controlled three-dimension growth with increasing nucleation rate, and diffusion-controlled growth with decreasing nucleation rate, respectively. Meanwhile, the values of n imply that the nucleation rate increases with increasing heating rate. Microstructure analysis indicates that the fabricated bulk alloys mainly consist of three kinds of crystallized phases, β-Ti, (Cu, Ni)–Ti_2, and Nb_3Sn, but exhibit different microstructures and mechanical properties. The effect of the heating rate on the microstructure and mechanical properties can be explained based on different crystallization mechanisms. Especially, obvious plasticity is resulted from formation of ductile $(Ti, Nb)_3Sn$ from the Nb_3Sn at relative high sintering temperature. The results obtained provide insight into fabrication of large-sized crystallized phase-containing bulk alloys with excellent mechanical property by powder metallurgy.

1. Introduction

As one of the most important engineering materials, titanium alloy has excellent mechanical properties and good corrosion resistance [1]. Improving strength and ductility of titanium alloys is always a significant topic in development of advanced structural materials. Among different fabrication routes, obtaining glassy structure is an effective route to improving strength. These obtained Ti-based bulk metallic glasses (MGs) can be classified into Beryllium-free and Beryllium-containing bulk MGs [2]. For the former case, their glass forming ability is limited and Ti concentration ($\leqslant$50 at.%) is relative low [3]. This causes their small critical size and relative low strength and specific strength, restricting their practical applications as lightweight engineering materials. For the latter case, although they exhibit higher glass forming ability and larger plasticity (1–5%) than those of the former ones, their strength are relative low compared with other bulk MGs [4]. Besides, as a kind of active alloying element, beryllium is easy to form toxic beryllium oxide during casting, which is harmful to our health.

Recently, a material forming method by coupling sintering of MG powder with crystallization of sintered bulk MG was introduced to fabricate Ti-based alloys with high strength and large ductility [5–13]. As for the material forming method, intrinsic relationship between crystallization mechanism of sintered bulk MG (or synthesized MG powder) and microstructure of sintered and crystallized bulk alloys is a significant academic topic involved. In our previous work, it was found that minor alloying substitution element, and minor varying content in the same alloying element can give rise to different nuclei growth mechanisms for synthesized MG powders and consequently cause different crystallized phases and microstructures of sintered and crystallized bulk alloys [14,15]. Also, according to the classical theory of nucleation and growth, we elucidated nucleation and growth mechanism of crystalline phase for fabrication of Ti-based bulk alloys with high strength and large ductility during crystallization of sintered bulk MG (or MG powder) [16–18]. Unfortunately, based on crystallization kinetics theory for a given alloy composition, little research has been focused on system studies about intrinsic relationship between crystallization mechanism of synthesized MG powder

* Corresponding author. Tel./fax: +86 20 87112111.
E-mail address: cyang@scut.edu.cn (C. Yang).

0925-8388/$ - see front matter © 2013 Elsevier B.V. All rights reserved.
http://dx.doi.org/10.1016/j.jallcom.2013.09.181

(or sintered bulk MG) and microstructure of sintered and crystallized bulk alloys.

In the present work, $Ti_{64}Nb_{12}Cu_{11.2}Ni_{9.6}Sn_{3.2}$ bulk alloys were fabricated by sintering of synthesized MG powder and crystallization of amorphous phase. The fabricated bulk alloys have high specific strength superior to those of Ti-based bulk MGs. The crystallization kinetics of the synthesized MG powder is investigated using the Johnson–Mehl–Avrami–Kolmogorov method. The aim of this work is to investigate the intrinsic relationship between the crystallization mechanism of the synthesized MG powder and the microstructure of the sintered and crystallized bulk alloys fabricated by powder metallurgy.

2. Experimental

$Ti_{64}Nb_{12}Cu_{11.2}Ni_{9.6}Sn_{3.2}$ MG powder was synthesized by mechanical alloying (MA). MA was conducted in a high-energy planetary ball mill (QM-2SP20, made by the apparatus factory of Nanjing University) with a mixture of pure Ti (−325 mesh, 99.5%), Nb (−325 mesh, 99.9%), Cu (−325 mesh, 99.9%), Ni (−325 mesh, 99.9%), and Sn (−325 mesh, 99.9%) powders. The powder mixtures with a stoichiometry of $Ti_{64}Nb_{12}Cu_{11.2}Ni_{9.6}Sn_{3.2}$ and stainless steel balls were placed in a stainless steel vial for MA. The diameters of the stainless steel balls were 15, 10, and 6 mm with a weight ratio of 1:3:1. The ball-to-powder mass ratio was approximately 12:1. MA was performed at a rotation speed of 4.3 s^{-1} under a protective argon atmosphere (99.999%, 0.5 MPa). Approximately 3 g of the milled powders were removed from the vial every 5 h for further examination. Subsequently, the synthesized MG powders were pre-compacted, sintered and then crystallized by spark plasma sintering (SPS) under an argon atmosphere by a Dr. Sintering SPS-825 system. The MG powders were first heated to 373 K in 3 min, followed by heating to different sintering temperatures (1123 K, 1173 K, and 1223 K) at different heating rates (50 K/min,100 K/min and 150 K/min) at a sintering pressure of 50 MPa and holding for different times (0 min, 5 min and 10 min). The sintered and crystallized bulk alloys had a cylindrical shape $\varnothing 20 \times 10$ mm.

The structural evolution of the milled powders for different milling times was confirmed by X-ray diffraction (XRD) (D/MAX-2500/PC; Rigaku Corp., Tokyo, Japan) with Cu Kα radiation. The thermal behavior of the milled powders was measured by differential scanning calorimetry (DSC) under a high-purity argon atmosphere at different heating rates. The phase constitution, microstructure, and uniaxial compression of the sintered and crystallized bulk alloys were characterized by XRD, SEM, TEM, and an MTS testing system. The detailed experimental procedures can be found in Refs. [5–16]. The XRD patterns were fitted using the attached Jade5 software to calculate the volume fraction of the β-Ti phase. The precise lattice parameters, a_0 and a_1 of the β-Ti and the Nb_3Sn phase in the sintered and crystallized bulk alloys were determined with an uncertainty of 10^{-5} nm using a suitable extrapolation of the variation in the lattice parameter as a function of the Nelson–Riley parameter $(\cos 2\theta/\sin\theta + \cos 2\theta/\theta)$ [19].

3. Results

Fig. 1A displays XRD patterns of the milled powders for different milling times. For the initial powder, XRD pattern exhibits all expected peaks of Ti, Nb, Cu, Ni and Sn elements (Fig. 1A(a)). With increasing milling time, the intensity of the peaks decreased and the width increased (Fig. 1A(b)–(e)). This can be ascribed to the reduction in grain size and the increase in lattice strain. Meanwhile, the major peak of α-Ti decreases gradually and the peaks of β-Ti emerges and increases (Fig. 1A(b)–(e)). This is resulted from the fact of α-Ti transforming into β-Ti solid solutions due to β-Ti formation elements Nb and Sn dissolved into the lattice of α-Ti during milling process. Prolonging the milling time to 25 h, all crystalline peaks disappear and only a broad diffraction peak exists at $2\theta = 39.0°$ (Fig. 1A(f)), indicating the formation of predominately glassy structure. Further high resolution TEM analysis confirms the existence of predominately glassy structure in the synthesized powder. As shown in Fig. 1B, the 25 h-milled alloy powder is mainly composed of glassy phase; while a small amount of β-Ti crystals with a size of 5–10 nm are distributed dispersedly in the glassy matrix. The synthesized MG powder provides the possibility of fabricating high-strength titanium alloys by the method of sintering and crystallization of amorphous phase.

To study the relationship between the crystallization mechanism of the synthesized $Ti_{64}Nb_{12}Cu_{11.2}Ni_{9.6}Sn_{3.2}$ MG powder and the microstructure and mechanical property of the sintered and crystallized bulk alloys fabricated by SPS and crystallization of amorphous phase, crystallization kinetics of the synthesized MG powder is discussed using the Johnson–Mehl–Avrami–Kolmogorov (JMAK) method [20]. The value of Avrami exponent $n(\alpha)$ reflects the crystallization mechanism at different temperatures or heating rates, which is applied to characterize the nucleation and growth behavior during the whole crystallization process. It can be used to explain the variation of the grain size and morphology after crystallization. In isothermal annealing experiments, $n(\alpha)$ can be deduced from the JMAK equation as follows [21]:

$$\alpha = 1 - \exp\left\{-[k(t-\tau)]^n\right\} \tag{1}$$

where α is the crystallized volume fraction which is a function of the time t; τ is a logarithmic time; n is the Avrami exponent and k is a kinetic coefficient which is a function of temperature. Given constant temperature, k is generally taken as a fixed value. Accordingly, JMAK equation can be rewritten as:

$$\ln[-\ln(1-\alpha)] = n\ln(t-\tau) + \text{const} \tag{2}$$

Plotting $\ln[-\ln(1-\alpha)]$ versus $\ln(t-\tau)$ will provide the n values from the slope of these curves. Furthermore, according to Eq. (2), $n(\alpha)$ can be determined by $\ln(t-\tau)$ derivation, as shown in the following equation:

$$n(\alpha) = \frac{d\ln[-\ln(1-\alpha)]}{d\ln(t-\tau)} \tag{3}$$

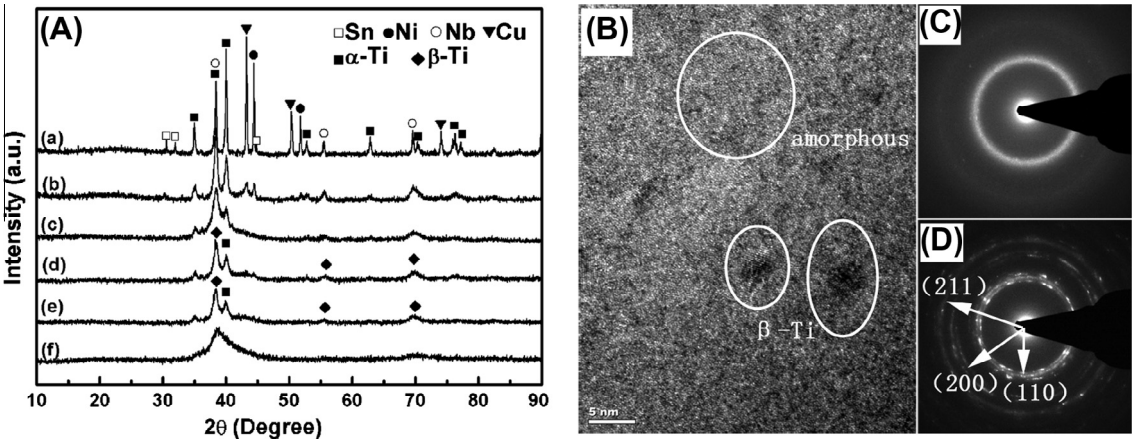

Fig. 1. (A) XRD patterns of the $Ti_{64}Nb_{12}Cu_{11.2}Ni_{9.6}Sn_{3.2}$ powders milled for different times: (a) 0 h, (b) 5 h, (c) 10 h, (d) 15 h, (e) 20 h, and (f) 25 h. (B) TEM bright-field image and corresponding selected area diffraction (SAD) patterns of the powder milled for 25 h.